Journal of Electronic Materials (2024) 53:4939–4946
https://doi.org/10.1007/s11664-024-11033-9

28TH INTERNATIONAL CONFERENCE ON NUCLEAR TRACKS AND RADIATION MEASUREMENTS

Highly Flexible, Selective and Sensitive Ammonia Sensor Based on MXene/Cellulose Nanofibers

Sagar Sardana[1] · **Aman Mahajan**[1]

Received: 15 December 2023 / Accepted: 6 March 2024 / Published online: 8 April 2024

Abstract
Flexible electronics have become imperative in an emerging era of the Internet of Things (IoT), as they offer promising alternatives to rigid and complex circuitry for the development of wearable devices. As a result, the research field of flexible gas sensors is increasingly being investigated, including different potential materials, with the aim of high selectivity and sensitivity. In this study, a flexible ammonia (NH_3) sensor unit was fabricated using cellulose nanofibers (C-NFs) as a flexible supporting framework and sensing material coating of $Ti_3C_2T_x$ MXene. The fabricated sensor displayed higher selectivity to NH_3 relative to other interferents in the ppm concentration range. The results revealed that the MXene/C-NFs-based sensor exhibited a response of 2.4% towards 5 ppm NH_3 with faster response and recovery times of 42 s and 69 s, respectively, which were improved relative to a pristine MXene-based sensor with sensing response of 1.42% and response/recovery time of 67 s/104 s. This enhanced sensing performance was ascribed to the large specific surface area and efficient charge transport pathways provided by the one-dimensional structure of C-NFs, which facilitated the surface adsorption/desorption of NH_3 molecules. In addition, the fabricated sensor demonstrated excellent flexibility features and reproducible sensing properties at different bending angles and bending cycles, with low sensing response attenuation of 5.2% under a maximum bending angle of 120°. Overall, this work illustrates the feasibility of employing a nanofiber matrix as a flexible sensing framework along with a porous absorption/desorption surface for next-generation wearable gas sensors.

Keywords MXene · cellulose · nanofibers · ammonia · sensor

Introduction

In recent years, the growing field of research on the two-dimensional (2D) inorganic material $Ti_3C_2T_x$ (MXene) has attracted tremendous attention in many device applications, including chemical gas sensors, solar cells, supercapacitors, diodes, and transistors.[1,2] In particular, in the field of chemical gas sensors, MXenes have become a potential and promising substitute for conventional metal-oxide semiconductors (MOS), which require elevated temperatures to operate, thus encountering high-power requirement issues.[3,4] In contrast, MXenes have emerged as a room-temperature sensing material owing to their exceptional properties including high conductance, high signal-to-noise ratio, large surface area, and tunable surface chemistry due to the presence of surface functional groups (–O, –OH, –F).[5,6] Notably, the theoretical insights into density functional theory simulations have revealed that MXene-based chemiresistive sensors are highly selective to NH_3.[7] NH_3 has been found to be an environmental toxin in chemical industries, agricultural fields, thermal power plants, and medical fields.[8,9] Additionally, NH_3 has been considered as a potential biomarker for diagnosis of diseases related to respiratory problems.[10] For instance, breath analysis has shown that NH_3 concentration in the exhaled breath of a healthy individual person is ~ 1 ppm.[11] Any change in this concentration suggests the presence of harmful respiratory diseases.[12] For this, there is an urgent need for the development of lightweight and flexible miniaturized gas sensors suitable for use as point-of-care devices.

In this regard, continuous efforts have been made towards the design of flexible geometry of MXene-based sensors, including: (i) utilization of potential deposition techniques;[13]

✉ Aman Mahajan
aman.phy@gndu.ac.in

[1] Material Science Lab, Department of Physics, Guru Nanak Dev University, Amritsar 143005, India

and (ii) strategic modification of MXene materials.[14] For instance, Yang et al.[15] used ultrasonic spray pyrolysis to develop a flexible sensor by modifying a 2D MXene structure into a 3D crumpled sphere, which in addition offered a large adsorption area for gas interaction and thus high sensing response. Quan et al.[16] utilized printing technology and fabricated a fully flexible MXene-based sensor on paper. Very recently, Nam et al.[5] fabricated a flexible MXene-based NH_3 sensor by directly coating the MXene materials onto flexible polyimide substrates, reporting long-term stability of the sensors even after 5000 bending cycles. On the other hand, the class of polymer materials has triggered an explosive expansion in the fabrication of flexible devices owing to their easy processability, flexibility, and lightweight properties.[17] In addition, the functional groups present on the surface of MXene facilitate interactions with polymer materials via electrostatic interactions, van der Waals interactions, and hydrogen bonding to form MXene/polymer composites. Owing to the multiple interactions between MXene and polymer materials, the abundant surface functionalities and hetero-interfacial contacts introduced into the materials significantly promote the interaction of NH_3 molecular composites.[18] Thus, polymer-based composites have been proven beneficial for the development of highly flexible and sensitive gas sensors. Cai et al.[19] fabricated a flexible NH_3 sensor based on MXene/urchin-like polyaniline composites deposited on a polyethylene terephthalate substrate, and reported enhanced sensing response of around 2% for 4 ppm NH_3. Likewise, other polymers including cellulose, polyacrylamide, PEDOT:PSS, polyvinyl alcohol, and polyethylenimine have shown great application prospects for enhancing the flexibility and sensing properties of MXene-based sensors.[18] Among them, cellulose has been found to be a more appropriate polymer material owing to its advantages including light weight, earth-abundance, high mechanical strength, and renewable and biodegradable nature.[20] Considering this, Cao et al.[21] developed ultrathin and highly flexible MXene/cellulose composite paper via layer-by-layer self-assembly using vacuum filtration. They revealed that the intercalation of cellulose material tightens the packing density, increases the mechanical strength, and resolves the restacking issues of MXenes. This kind of self-assembly of layered MXene/polymer composite material holds great potential for sensing properties by retaining the conductivity of MXenes and the flexible platform of polymer material.

Considering the aforementioned discussion, in the present work, a flexible NH_3 sensor was constructed using a sensing framework of cellulose nanofibers (C-NFs) processed through electrospinning followed by loading of MXene sensing material through a dip-coating process. We obtained the MXene/C-NF layered composite with a backbone of scalable open pore channels of C-NFs in which MXene sheets were adhered in a controlled manner, addressing issues related to restacking and aggregation of MXene sheets. More importantly, owing to their one-dimensional structure, C-NFs provide a high surface-to-volume ratio and efficient charge transport pathways, facilitating the adsorption/desorption properties of NH_3 molecules on the MXene surface and hence improving the sensing properties of the MXene. In addition, the biodegradable nature of C-NFs in this sensing framework meets the demand for eco-friendly materials for flexible and wearable electronic systems.

Experimental Part

Materials

MAX phase Ti_3AlC_2 precursor was obtained from Nanoshel UK Ltd. Cellulose acetate (M_W: 30,000) and sodium hydroxide (NaOH) were purchased from Merck, India. The solvents including hydrofluoric acid (HF; 38% concentrated), acetone, *N*,*N*-dimethylformamide (DMF), and deionized (DI) water were of analytical grade.

Synthesis of MXene

The HF-etching method was used to synthesize the MXene.[22] First, 1 g of MAX precursor was gradually added in small proportions into 20 mL HF and stirred continuously for 24 h at room temperature. The resulting etched product was then centrifuged at 3500 rpm until the pH of the supernatant reached ~ 6. The obtained product was added to ethanol and sonicated in an ice bath (−5°C) for 1 h to obtain delaminated MXene sheets. Subsequently, the final product was collected by vacuum-assisted filtration followed by drying in an oven at 60°C for 24 h.

Preparation of Cellulose Nanofibers (C-NFs)

First, a polymeric solution of cellulose acetate (CA) was prepared by adding 2.85 g of CA into 15 mL of acetone/DMF (volume ratio of 2:1) solution. The resultant transparent and viscous solution was filled into a 5-mL syringe and placed in an electrospinning chamber. The parameters were set with a pump flow rate of 0.7 µL/s, high voltage supply of 17 kV, and tip-to-collector distance of 15 cm. The as-spun NFs were collected on polyimide sheets pre-coated with Ag interdigital electrodes. Further, to obtain C-NFs, the prepared CA-NFs deposited on polyimide sheets were immersed into 0.1 M NaOH solution for 36 h for deacetylation, which was followed by a cleaning process with DI water.[23]

Fabrication of the Sensor and Gas Sensing Measurements

The pristine MXene-based sensor was prepared by simply drop-casting the MXene aqueous solution (0.1 g/mL) onto a polyimide sheet pre-coated with Ag interdigital electrodes. For the MXene/C-NF-based sensor, the regenerated C-NFs deposited on polyimide sheets were immersed into MXene aqueous solution (0.1 g/mL) and kept for overnight drying. Further, to study the gas sensing properties, the prepared sensor was placed into a 1 L stainless-steel chamber with metal pressure contact equipped with Keithley source meter probes (Agilent B2902A). An Owlstone Vapor Generator (OVG-4) was used to create the vapor exposure of targeted gases using the pre-calibrated permeation tubes. The parameters of the OVG-4 system including flow rate, permeation rate, temperature, and dry air as carrier gas at different mixing ratios were used to obtain the desired concentration of sample gases (Table I).

The gas response (%) was calculated by determining the ratio of absolute change in resistance of the sensing material in target gas and air to the baseline resistance in air as Eq. 1.[24]

$$\text{Response}\,(\%) = \frac{R_g - R_a}{R_a} \times 100 \tag{1}$$

where R_g and R_a are the resistance of the sensing material in the target gas and air, respectively.

Characterization Tools

A grazing incidence x-ray diffraction instrument (GIXRD; Bruker D8 Focus) equipped with Cu-$K_{\alpha 1}$ radiation of wavelength $\lambda = 1.5406$ Å operated at 40 kV and 30 mA was used to study the crystallographic information of samples. Field-emission scanning electron microscopy (FESEM; Carl Zeiss, Supra 55) was used to study the surface morphology of samples. The specific surface area of samples was evaluated by the Brunauer-Emmett-Teller (BET) technique (surface area and porosity analyzer, Micrometrics ASAP 2020).

Table I Parameters of the Owlstone Vapor Generator to produce different NH_3 concentrations

Flow rate (mL/min)	Temperature (°C)	Gas concentration (ppm)
50	30	~1
100	40	~3
500	50	~5
500	60	~10
500	65	~15

Results and Discussion

XRD patterns shown in Fig. 1 reveal the crystallographic information of C-NFs and MXene/C-NFs. The XRD pattern contains a broad peak between 15° and 25° indexed to the (200) plane of C-NFs along with constant background noise, which indicates the amorphous nature of the sample. This could be attributed to the electrospinning process, where the applied high electric field constrained the flow-induced molecular orientation of molecular chains of the processed sample,[25] resulting in crystallinity loss of C-NFs. The XRD pattern of MXene/C-NFs shows changes in the crystallite structure of C-NFs after MXene loading, where the diffraction peaks at 9.24°, 18.11°, and 25.18° correspond to (002), (004), and (006) characteristic planes of the MXene. Notably, by dip-coating, the loading of MXene on the surface of C-NFs increases the crystallinity of MXene/C-NFs, as evident from intensity loss of broad peak and background noise.

To explore the surface morphological structures of C-NFs and MXene/C-NFs, FESEM analysis was conducted. Figure 2a shows the FESEM image of C-NFs, depicting the randomly oriented and bead-free nanofibrous structure. The average diameter of C-NFs was evaluated to be 720 nm using Image J1.29X software. Of note, during the electrospinning process, the nanofibers tend to be self-assembled in such a way that leads to micro-sized void formation between the fibers. Figure 2b shows the FESEM image of MXene/C-NFs, depicting the coverage of MXene on surface as well as void occupation sites of C-NFs. It is noteworthy that the

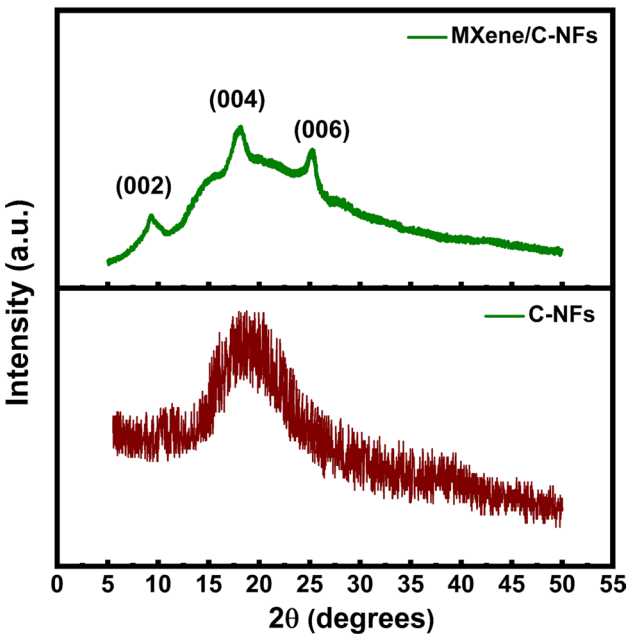

Fig. 1 XRD patterns of C-NFs and MXene/C-NFs.

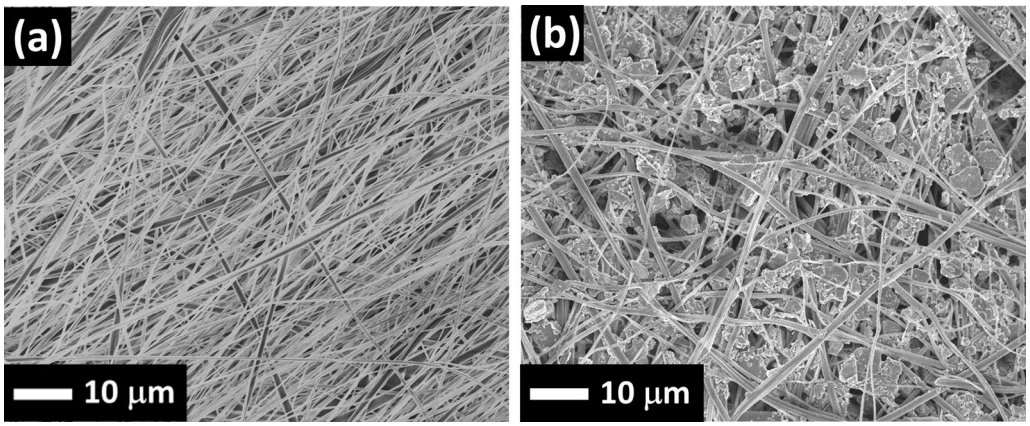

Fig. 2 FESEM images of (a) C-NFs and (b) MXene/C-NFs.

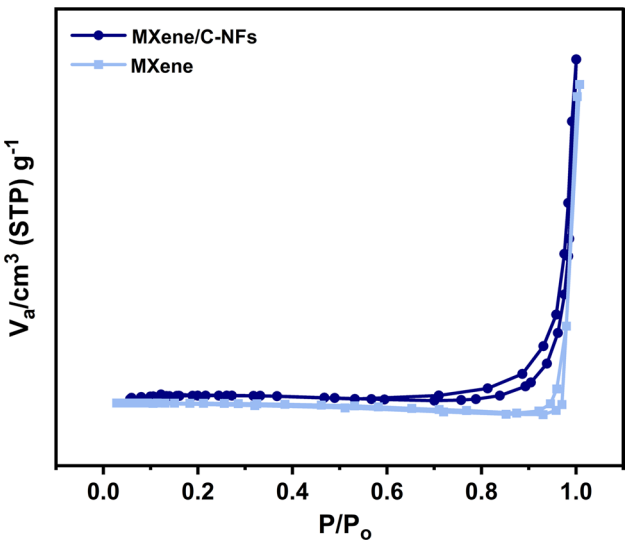

Fig. 3 BET analysis of pristine MXene and MXene/C-NFs.

–OH rich sites of C-NFs hold the MXene tightly by forming strong hydrogen bonding through surface termination groups of MXene. This type of closely packed nanofibrous structure possesses high specific surface area for adsorption properties and strong mechanical strength for high flexibility.

BET analysis was conducted to assess the contribution of C-NF substrate on the specific surface area of composite sample. Figure 3 shows the N_2 adsorption-desorption isotherm plots of MXene/C-NFs with MXene as reference sample. The isotherm plots of both the samples are characterized by a type IV isotherm curve with H3-type hysteresis loop, demonstrating the mesoporous structure. The results of the MXene/C-NFs isotherm curve revealed a fourfold enhanced specific surface area of 15.86 m^2/g compared to pristine MXene (3.92 m^2/g). This was attributed to the electrospun porous C-NF substrate, which serves the large specific surface area and high porosity, resulting in a high surface-to-volume ratio. Thus, it is expected to achieve enhanced sensing performance for MXene/C-NFs compared to pristine MXene.

Further, the room-temperature NH_3 sensing experiments were conducted to evaluate the impact of C-NF substrate on the sensing performance of MXene. For this, the two distinct sensors were constructed based on (i) pristine MXene and (ii) MXene/C-NFs. Both were deposited onto the polyimide sheets pre-coated with Ag interdigital electrodes. To evaluate the gas sensing ability, each sensor was exposed to 5 ppm NH_3 at room temperature (Fig. 4a). The MXene/C-NF-based sensor exhibited an enhanced sensing response of 2.4% compared to pristine MXene sensing response of ~ 1.42%. The enhanced sensing response of MXene/C-NFs is attributed to the high specific surface area (15.86 m^2/g) supported by C-NFs, which led to greater exposure of active sites of MXene for interaction of NH_3 molecules and thereby enhanced sensing response. Meanwhile, the limited sensing response of the pristine MXene-based sensor could be due to restacking of MXene material when directly deposited onto polyimide sheets which hampers the charge-transfer process during gas interaction. Further, the comprehensive response/recovery properties of the prepared sensors were evaluated. The MXene-based sensor exhibited response and recovery times of 67 s and 104 s, respectively. In contrast, the MXene/C-NF-based sensor exhibited quicker response and recovery times of 42 s and 69 s, respectively, due to fast adsorption/desorption properties of hybrid nanofibrous networks.

For selectivity analysis of MXene/C-NFs, the investigation of the prepared sensor was extended to different gases including ammonia, ethanol, acetone, methanol, isopropanol, carbon dioxide, and chlorine each at 5 ppm. Figure 4b shows the polar plot of corresponding responses, representing the highest selectivity to NH_3 among others. For

comparison, we also examined the response of the pristine MXene-based sensor for all gases and observed the similar selectivity behavior of MXene which can be ascribed to strong adsorption properties of MXene towards NH_3 molecules according to density functional theory calculations. The calculated response (%) values of MXene and MXene/C-NFs based sensor were evaluated and compared in histogram plot (Fig. 4c), indicating the higher response changes for MXene/C-NFs based sensor for all gases.

Further, the sensing performance of the MXene/C-NF-based sensor was recorded for NH_3 gas covering the concentration range from 1 ppm to 15 ppm. The resistance-time curves for 1 ppm, 3 ppm, 5 ppm, 10 ppm, and 15 ppm NH_3 are plotted in Fig. 4d, depicting the increased resistance changes with increasing NH_3 concentration with excellent sensor recovery. In connection, the corresponding sensor responses were evaluated and fitted in Eq. 2 [26] as shown in Fig. 4e.

$$S(\%) = A_g P_g^{\beta} \tag{2}$$

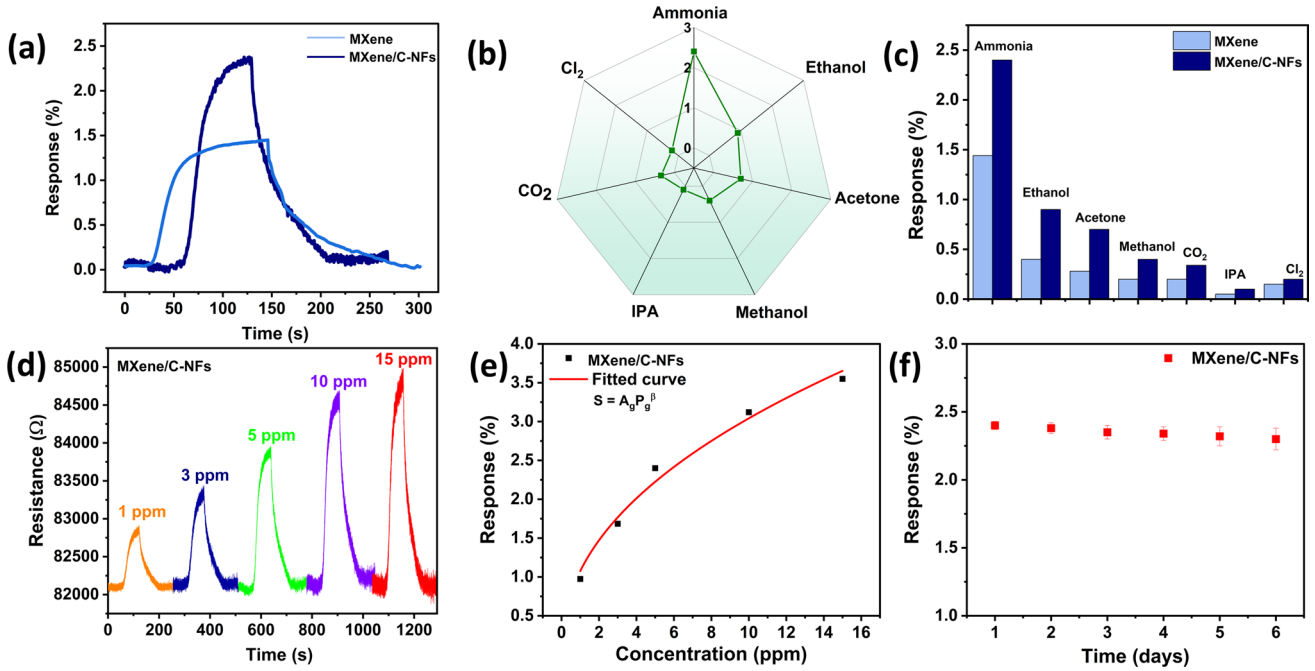

Fig. 4 (a) Comparative response of pristine MXene and MXene/C-NF-based sensor. (b) Polar plot representing the selectivity of the MXene/C-NF-based sensor. (c) Histogram showing the comparative response analysis of pristine MXene and the MXene/C-NF-based sensor. (d) Resistance-time curves and (e) the corresponding responses of the MXene/C-NF-based sensor towards different concentrations of NH_3. (f) Stability test of the MXene/C-NF-based sensor.

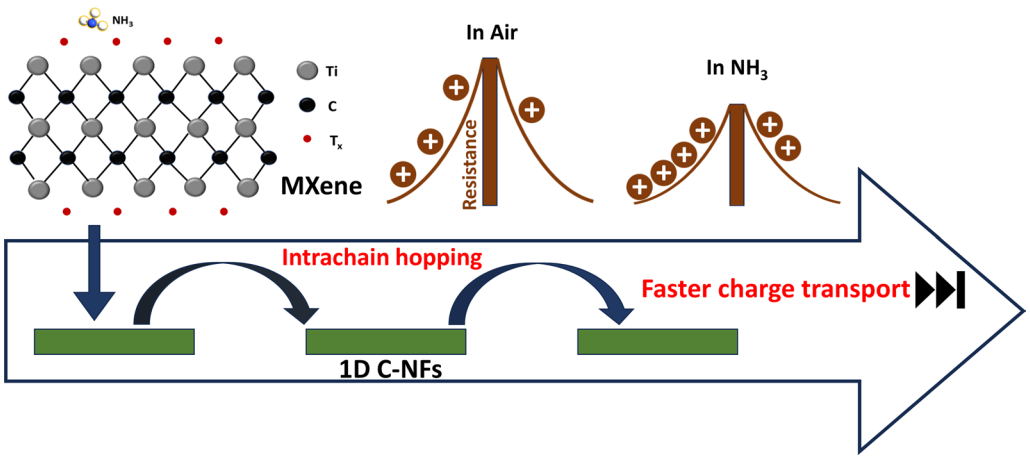

Fig. 5 Schematic of gas sensing mechanism of the MXene/C-NF-based sensor with specific roles of MXene and C-NFs.

where S (%) is sensor response, A_g represents pre-factor and P_g defines gas partial pressure proportional to gas concentration. The factor β is defined as the response exponent with an ideal value of 0.5, which describes the gas sensing phenomenon. Herein, the β value is estimated to be 0.45, attributing to the fact that the NH_3 interaction with MXene/C-NFs is a surface phenomenon. Further, a stability test of the MXene/C-NF-based sensor was conducted, and the recorded sensing response towards 5 ppm $NH_3$for 1–6 days is shown in Fig. 4f. The gas response remained almost stable with only slight attenuation, indicating good stability of the sensor.

Unlike metal-oxide-based sensors, herein, the chemiresistive effect is independent of the oxidizing and reducing properties of gases, showcasing an increased change in resistance, which is governed by inherent metallic properties of MXene. The surface functional groups of MXene play a vital role in sensing properties. The adsorption of gas molecules takes place on surface defect sites of MXene through interaction with surface functional groups (Fig. 5). On one hand, the surface functional groups offer high electronegativity leading to strong surface adsorption of gases through hydrogen bonding and thus high sensing response. On the other hand, the robust electron shielding effect hinders the carrier-charge exchange of MXene with gas molecules resulting in longer response-recovery times for the pristine MXene-based sensor. In contrast, the MXene/C-NF-based sensor showed improved sensing properties that could be attributed to the high specific surface area along with the numerous scalable open pore channels provided by C-NFs, which enable higher loading capacity of sensing materials for superior gas adsorption and diffusion properties. Additionally, the 1D structure of the C-NF matrix provides efficient charge carrier transport pathways to conduct sensing signals via prominent intra-chain hopping processes (Fig. 5), resulting in fast response/recovery times.

A comparison of sensing results of the as-fabricated sensor in the present work and previously reported sensors based on MXene is tabulated (Table II). Further, the exceptional selectivity of the MXene-based sensor towards NH_3 gas has been theoretically demonstrated by density functional theory (DFT) calculations in the previous reports.[7,27,28] The derived DFT simulations revealed that $Ti_3C_2T_x$ MXene has good adsorption properties towards NH_3. The high electron cloud density around the N atoms in NH_3 leads to greater interaction with the MXene sensing layer and thereby, high selectivity for NH_3. Meanwhile, NH_3 has lighter molecular weight, i.e., 17.03 g/mol, than the other tested gases including ethanol (46.068 g/mol), acetone (58.08 g/mol), methanol (32.04 g/mol), isopropanol (60.1 g/mol), carbon dioxide (44.01 g/mol), and chlorine (35.5 g/mol), which promotes the diffusion of NH_3 molecules based on Knudsen diffusion theory (Eq. 3).[29]

$$D_K = \frac{3r}{4}\sqrt{\frac{2RT}{\pi M}} \tag{3}$$

where D_K is the Knudsen diffusion constant, r is the pore radius, T is the temperature, and M is the molecular weight. In this way, MXene coated on a C-NF substrate offered superior sensing performance towards NH_3 relative to other gases.

To comply with the practical applications, the flexibility of the prepared sensor is demonstrated in Fig. 6a. Further, to test the impact of flexibility on sensing performance of the MXene/C-NF-based sensor, the gas sensing responses were measured at 5 ppm NH_3 gas under different bending states. The calculated sensing responses (%) and their corresponding attenuations (%) are displayed in Fig. 6b. Under the maximum bending angle of 120°, the sensing response of the MXene/C-NF-based sensor was reduced by 5.2%, indicating that the MXene/C-NFs had excellent bending capability with acceptable attenuation. Furthermore, the stability test under the bending state was conducted, where the bending angle was fixed to 90°. The response attenuations were found to 5.8%, 6.7%, 10.5%, and 13.8% after repeating bending cycles of 50, 100, 500, and 1000 (Fig. 6c). This shows that the sensing performance of the prepared MXene/C-NF-based sensor is favorable even after bending for several cycles, showing the great application prospects of prepared sensing framework of C-NFs for wearable sensors.

Table II Comparison of NH_3 sensing performance based on present sensor and previous works

Sensing material	Substrate	Concentration (ppm)	Response (%)	Response/recovery time	References
MXene	Rigid	10	0.8	~36 s/80 s	7
MXene	Rigid	5	0.62	~4 min/3 min	30
MXene	Rigid	100	0.8	~3.5 min/6 min	31
3D MXene framework	Flexible	10	0.7	~1–2 min/4–5 min	32
MXene/Polyacrylamide	Flexible	50	1.5	~8 s/5 s	33
MXene/C-NFs	Flexible	5	2.4	42 s/69 s	This work

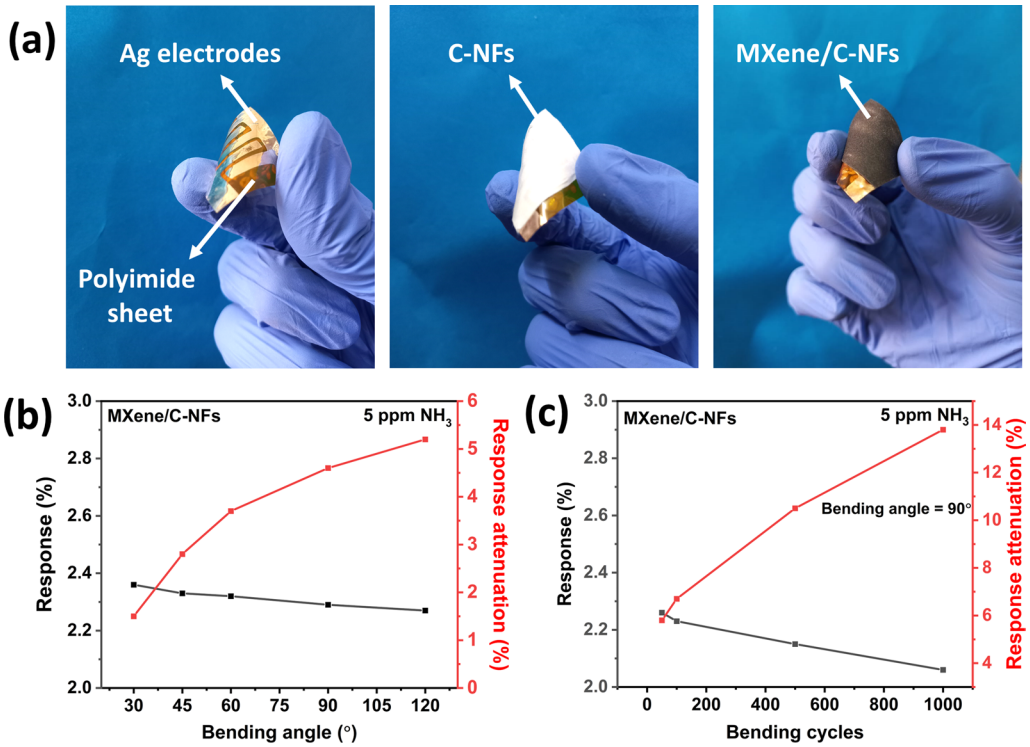

Fig. 6 (a) Photographs showing the flexibility and bendability of the prepared sensor. Responses (%) of the MXene/C-NF-based sensor at 5 ppm NH_3 (b) at different bending angles and (c) after different bending cycles with their attenuation (%) relative to response (%) in the unbent state.

Conclusions

In summary, we have developed a flexible NH_3 sensor by utilizing electrospun C-NFs as supporting framework and MXene as a sensing material. The use of C-NFs not only provided a high specific surface area but also facilitated the transfer of charge carriers for faster response and recovery properties. The study findings confirmed that the MXene/C-NF-based sensor showed enhanced sensing response of 2.4% towards 5 ppm NH_3 along with faster response/recovery times of 42 s/69 s relative to a pristine MXene-based sensor with sensing response of 1.42% and response/recovery times of 67 s/104 s. Further, the prepared sensor showed excellent flexibility towards different bending angles and bending cycles while retaining the gas sensing performance with small acceptable attenuation. Notably, the proposed approach holds great application prospects for the development of wearable sensors for both environmental and health monitoring.

Acknowledgements One of the authors (S.S.) is grateful to DST INSPIRE, New Delhi, for providing a fellowship.

Conflict of interest The authors have no conflicts to disclose.

References

1. Z. Cui, C. Gao, Z. Fan, J. Wang, Z. Cheng, Z. Xie, Y. Liu, and Y. Wang, Breathable, durable and bark-shaped MXene/textiles for high-performance wearable pressure sensors, EMI shielding and heat physiotherapy. *J. Electron. Mater.* 50, 2101 (2021).
2. M. Cao, F. Wang, L. Wang, W. Wu, W. Lv, and J. Zhu, Room temperature oxidation of Ti_3C_2 MXene for supercapacitor electrodes. *J. Electrochem. Soc.* 164, A3933 (2017).
3. A. Mirzaei, M. Lee, H. Safaeian, T.U. Kim, J.Y. Kim, and S. Kim, Room temperature chemiresistive gas sensors based on 2D MXenes. *Sensors* 23, 8829 (2023).
4. Y. Seekaew, S. Kamlue, and C. Wongchoosuk, Room-temperature ammonia gas sensor based on $Ti_3C_2T_x$ MXene/graphene oxide/CuO/ZnO nanocomposite. *ACS Appl. Nano Mater.* 6, 9008 (2023).
5. M.S. Nam, J.Y. Kim, A. Mirzaei, M.H. Lee, H.W. Kim, and S.S. Kim, Au- and Pt-decorated $Ti_3C_2T_x$ MXenes for preparing self-heated and flexible NH_3 gas sensors. *Sens. Act. B Chem.* 403, 135112 (2023).
6. R. Bhardwaj and A. Hazra, MXene-based gas sensors. *J. Mater. Chem. C Mater.* 9, 15735 (2021).
7. M. Wu, M. He, Q. Hu, Q. Wu, G. Sun, L. Xie, Z. Zhang, Z. Zhu, and A. Zhou, Ti_3C_2 MXene-based sensors with high selectivity for NH_3 detection at room temperature. *ACS Sens.* 4, 2763 (2019).
8. A. Raza, R. Abid, I. Murtaza, and T. Fan, Room temperature NH_3 gas sensor based on PMMA/RGO/ZnO nanocomposite films fabricated by in-situ solution polymerization. *Ceram. Int.* 49, 27050 (2023).
9. A. Kumar, R. Kashyap, R. Kumar, R. Singh, B. Prasad, M. Kumar, and D. Kumar, Experimental and numerical modelling

of a nanostructured nickel ferrite-based ammonia gas sensor. *J. Electron. Mater.* 51, 4040 (2022).
10. S. Sardana, H. Kaur, B. Arora, D.K. Aswal, and A. Mahajan, Self-powered monitoring of ammonia using an MXene/TiO_2/cellulose nanofiber heterojunction-based sensor driven by an electrospun triboelectric nanogenerator. *ACS Sens.* 7, 312 (2022).
11. H.Y. Li, C.-S. Lee, D.H. Kim, and J.-H. Lee, Flexible room-temperature NH_3 sensor for ultrasensitive, selective, and humidity-independent gas detection. *ACS Appl. Mater. Interfaces* 10, 27858 (2018).
12. S. Sardana and A. Mahajan, Edge-site-enriched $Ti_3C_2T_x$ MXene/MoS_2 nanosheet heterostructures for self-powered breath and environmental monitoring. *ACS Appl. Nano Mater.* 6, 469 (2022).
13. S.P. Sreenilayam, I. Ul Ahad, V. Nicolosi, and D. Brabazon, MXene materials based printed flexible devices for healthcare, biomedical and energy storage applications. *Mater. Today* 43, 99 (2021).
14. R.B. John, V. Karthikeyan, N. Septiani, A. Hardiansyah, A.R. Kumar, B. Yuliarto, and A. Hermawan, Gas-sensing mechanisms and performances of MXenes and MXene-based heterostructures. *Sensors* 23, 8674 (2023).
15. Z. Yang, S. Lv, Y. Zhang, J. Wang, L. Jiang, X. Jia, C. Wang, X. Yan, P. Sun, Y. Duan, F. Liu, and G. Lu, Self-assembly 3D porous crumpled MXene spheres as efficient gas and pressure sensing material for transient all-MXene sensors. *Nanomicro Lett.* 14, 56 (2022).
16. W. Quan, J. Shi, H. Luo, C. Fan, W. Lv, X. Chen, M. Zeng, N. Hu, Y. Su, H. Wei, and Z. Yang, Fully flexible MXene-based gas sensor on paper for highly sensitive room-temperature nitrogen dioxide detection. *ACS Sens.* 8, 103 (2023).
17. W. Yang, Y. Qin, Z. Wang, T. Yu, and Z. Ge, Recent Advances in the development of flexible sensors: mechanisms, materials, performance optimization, and applications. *J. Electron. Mater.* 51, 6735 (2022).
18. V. Chaudhary, A. Gautam, Y. Mishra, and A. Kaushik, Emerging MXene–polymer hybrid nanocomposites for high-performance ammonia sensing and monitoring. *Nanomaterials* 11, 2496 (2021).
19. Y. Cai, Y. Wang, X. Wen, J. Xiong, H. Song, Z. Li, D. Zu, Y. Shen, and C. Li, $Ti_3C_2T_x$ MXene/urchin-like PANI hollow nanosphere composite for high performance flexible ammonia gas sensor. *Anal. Chim. Acta* 1225, 340256 (2022).
20. Z. Zhou, Q. Song, B. Huang, S. Feng, and C. Lu, Facile fabrication of densely packed Ti_3C_2 MXene/nanocellulose composite films for enhancing electromagnetic interference shielding and electro-/photothermal performance. *ACS Nano* 15, 12405 (2021).
21. W.T. Cao, F.F. Chen, Y.J. Zhu, Y.G. Zhang, Y.Y. Jiang, M.G. Ma, and F. Chen, Binary strengthening and toughening of MXene/cellulose nanofiber composite paper with nacre-inspired structure and superior electromagnetic interference shielding properties. *ACS Nano* 12, 4583 (2018).
22. M. Alhabeb, K. Maleski, B. Anasori, P. Lelyukh, L. Clark, S. Sin, and Y. Gogotsi, Guidelines for synthesis and processing of two-dimensional titanium carbide ($Ti_3C_2T_x$ MXene). *Chem. Mater.* 29, 7633 (2017).
23. Z. Pang, Z. Yang, Y. Chen, J. Zhang, Q. Wang, F. Huang, and Q. Wei, A room temperature ammonia gas sensor based on cellulose/TiO_2/PANI composite nanofibers. *Colloids Surf A Physicochem Eng Asp* 494, 248 (2016).
24. A.S. Khune, V. Padghan, R. Bongane, V.N. Narwade, B.N. Dole, N.N. Ingle, M.L. Tsai, T. Hianik, and M.D. Shirsat, Highly selective chemiresistive SO_2 sensor based on a reduced graphene oxide/porphyrin (rGO/TAPP) composite. *J. Electron. Mater.* 52, 8108 (2023).
25. G.V.N. Rathna, J.P. Jog, and A.B. Gaikwad, Development of non-woven nanofibers of egg albumen-poly (vinyl alcohol) blends: influence of solution properties on morphology of nanofibers. *Polym. J.* 43, 654 (2011).
26. R.W.J. Scott, S.M. Yang, G. Chabanis, N. Coombs, D.E. Williams, and G.A. Ozin, Tin dioxide opals and inverted opals: near-ideal microstructures for gas sensors. *Adv. Mater.* 13, 1468 (2001).
27. X. Tian, L. Yao, X. Cui, R. Zhao, T. Chen, X. Xiao, and Y. Wang, A two-dimensional $Ti_3C_2T_X$ MXene@TiO_2/MoS_2 heterostructure with excellent selectivity for the room temperature detection of ammonia. *J. Mater. Chem. A Mater.* 10, 5505 (2022).
28. K. Weng, J. Peng, Z. Shi, A. Arramel, and N. Li, Highly NH_3 sensitive and selective $Ti_3C_2O_2$-based gas sensors: a density functional theory-NEGF study. *ACS Omega* 8, 4261 (2023).
29. M. Liu, J. Ji, P. Song, J. Wang, and Q. Wang, Sensing performance of α-Fe_2O_3/$Ti_3C_2T_x$ MXene nanocomposites to NH_3 at room temperature. *J. Alloys Compd.* 898, 162812 (2022).
30. C.E. Shuck, M. Han, K. Maleski, K. Hantanasirisakul, S.J. Kim, J. Choi, W.E.B. Reil, and Y. Gogotsi, Effect of Ti_3AlC_2 MAX phase on structure and properties of resultant $Ti_3C_2T_x$ MXene. *ACS Appl. Nano Mater.* 2, 3368 (2019).
31. S.J. Kim, H.-J. Koh, C.E. Ren, O. Kwon, K. Maleski, S.Y. Cho, B. Anasori, C.-K. Kim, Y.-K. Choi, J. Kim, Y. Gogotsi, and H.-T. Jung, Metallic $Ti_3C_2T_x$ MXene gas sensors with ultrahigh signal-to-noise ratio. *ACS Nano* 12, 986 (2018).
32. W. Yuan, K. Yang, H. Peng, F. Li, and F. Yin, A flexible VOCs sensor based on a 3D Mxene framework with a high sensing performance. *J. Mater. Chem. A Mater.* 6, 18116 (2018).
33. L. Zhao, Y. Zheng, K. Wang, C. Lv, W. Wei, L. Wang, and W. Han, Highly stable cross-linked cationic polyacrylamide/$Ti_3C_2T_x$ MXene nanocomposites for flexible ammonia-recognition devices. *Adv. Mater. Technol.* 5, 2000248 (2020).